DOI: 10.13009/EUCASS2025-515
11TH EUROPEAN CONFERENCE FOR AERONAUTICS AND SPACE SCIENCES (EUCASS)

Design and Testing of a Three-Surface Demonstrator with Redundant Longitudinal Control

Stefano Cacciola⋆†*, Carlo Fazioli*⋆*, Leonardo Filippello*⋆ *and Carlo E.D. Riboldi*⋆
⋆*Department of Aerospace Science and Technology, Politecnico di Milano*
Via La Masa 34 - 20156 Milan, Italy
stefano.cacciola@polimi.it
†Corresponding Author: Stefano Cacciola, stefano.cacciola@polimi.it

Abstract

Improvements in aviation are typically driven by innovative propulsion systems and unconventional configurations. However, these novel technologies require significant changes in the way we design, build, and operate aircraft. For instance, the widespread use of hydrogen in civil aircraft engines would necessitate substantial modifications to the supply chain and storage systems at airports. In this context, intelligent adaptations of conventional configurations may offer a viable alternative. Three-surface airplanes have often been considered as potential alternatives to standard designs with a conventional tail and elevator degree of freedom. Recently,[2,3] a three-surface configuration was employed to demonstrate the potential benefit of the redundant longitudinal control: when both the canard and tail have a movable part, the longitudinal trim, i.e. the balance of vertical forces and pitch moments, becomes overdetermined. As a result, an infinite number of canard and elevator deflections can trim the airplane, allowing the identification of control combinations that also minimize the overall drag of the airplane across all possible flight conditions. As reported in preliminary work,[3] a comparison between a standard back-tailed four-seat propeller-driven aircraft and an equivalent three-surface aircraft with redundant longitudinal control predicted that the latter configuration offers a 4% improvement in the maximum lift-to-drag ratio, potentially leading to comparable fuel savings with only a relatively minor change to the airframe design. Building on this promising analysis, we have developed a flying prototype to demonstrate the effectiveness of three-surface configuration with redundant longitudinal control. To achieve this, we first created a reference back-tailed prototype designed for a standard mission of a remote-controlled scaled airplane. Next, we developed an equivalent three-surface aircraft, with the same wing, static margin, and empennage volume. To achieve this, when a canard of a specific area is added to the aircraft, the tail area must be reduced and the wing shifted backward. Both the canard and tail are equipped with movable surfaces, introducing redundancy in the longitudinal trim. This redundancy is leveraged to minimize drag across all speeds, resulting in a quasi-linear relationship between the canard and elevator deflections. The size and incidence of the canard were optimized to maximize the lift-to-drag ratio of the trimmed polar. The results obtained through the flight testing campaign showed an increase in the maximum lift-to-drag ratio of about 10% when passing from a standard back-tailed airplane to an equivalent three-surface one with redundant longitudinal control.

1. Introduction

Aircraft designs incorporating three lifting surfaces have long been explored by aeronautical engineers as a viable alternative to traditional aft-tailed configurations. Historically, this layout has been regarded as an efficient solution, as demonstrated by the Piaggio P180[7] and supported by various studies highlighting its benefits in enhancing trim efficiency[6,13] and mitigating flutter in highly flexible airframes.[10]

Nevertheless, this configuration has never surpassed conventional two-surface designs in widespread adoption, probably because of the intrinsic complexity of aerodynamic interaction between multiple surfaces.[1]

In recent studies,[2,3,9] a three-surface layout was utilized to highlight the advantages of redundant longitudinal control. When both the canard and the tail feature movable control surfaces, the longitudinal trim — defined by the equilibrium of vertical forces and pitching moments — becomes an overconstrained problem. This condition enables ideally infinite combinations of canard and elevator deflections to achieve trim, making it possible to select some optimal configurations, for example, the one that also reduces the aircraft trimmed drag under various flight conditions.

DOI: 10.13009/EUCASS2025-515

Building upon these encouraging findings, we developed a flying platform to validate the performance of a three-surface configuration featuring redundant longitudinal control. The process began with the design and built of a conventional aft-tailed prototype tailored for a typical mission profile of a radio-controlled scale aircraft. Afterwards, an equivalent three-surface version was then created, maintaining the same wing design, static margin, and tail volume. This clearly required adjusting the layout: introducing a canard of a defined area necessitated a corresponding reduction in tail size and a rearward shift of the wing. Both the canard and tail were fitted with movable control surfaces, thereby enabling redundancy in achieving longitudinal trim.

The flying platform configurable as a two- or three-surface airplane is named “Aether”.

The design process for both Aether prototypes utilized Digital Datcom and specialized downwash/upwash models[4,5] to determine the aerodynamic characteristics of the reference and equivalent three-surface aircraft.

The two prototypes were tested starting from March 2025 with the following goals:

- Find the stall speed of both airplanes through the usual procedure.
- Find the location of the neutral point of both prototypes
- Estimate the polar of the two-surface airplane
- Estimate the polar of the three-surface airplane for different deflections of the canard control surface

The comparison of the estimated drag polars revealed that the three-surface aircraft with redundant longitudinal control achieves a maximum lift-to-drag ratio approximately 10% higher than that of the equivalent two-surface configuration.

2. Design of the Aether platform to study the performance of three-surface airplane with redundant longitudinal control

The goal of the present section is to describe the procedure followed to design a three-surface airplane with redundant longitudinal control equivalent to a reference back-tailed one. The equivalence is formulated in terms of two main parameters of the flight mechanics, which are strongly connected to the equilibrium, stability and maneuverability: the static margin and the tail volume. In particular, starting from an existing back-tailed aircraft, the equivalent three-surface version retains the same wing and static margin, while the total empennage volume, defined as the combined volume of the tail and canard, is matched to the tail volume of the reference aircraft.

Moreover, the prototypes were designed with a dual objective: to closely resemble existing civil passenger aircraft and to enable a direct comparison of the aerodynamic performance between two-surface and three-surface configurations. As a result, unconventional layouts that might offer particularly high performance for scaled, remotely piloted aircraft were intentionally excluded from consideration. More broadly, the design of the reference aircraft consistently aimed to find a balance between the objectives mentioned above and the optimization of the overall configuration.

2.1 Design of the reference two-surface airplane

The design of the two-surface airplane started from the traditional process reported in Roskam approach[11] and based on the sizing matrix plot, through which it was possible to select the wing and power loading equal respectively to about 11.2 kg/m^2 and 11.7 kg/kW.

The mass of the airframe and that of motor were preliminarily estimated through statistical regression, as well as the value of the expected parasite drag C_{D0}. The value of the wing aspect ratio was selected as the average of the data available in Roskam,[11] specifically regarding both subsonic jet and large turboprop. The chosen value for the aspect ratio is 7.2, which is not extremely high, but is associated with a good level of aerodynamic performance without increasing structural loads. It was additionally decided to set a null sweep angle at the trailing edge, in order to facilitate the arrangement of the actuators for the control surfaces. With this constraint, the wing sweep angle resulted in being uniquely linked to the taper ratio.

The design of the wing was constrained by two important aspects. First, given the small size of the prototypes, the low and varying Reynolds numbers during flight tests were expected to significantly alter the aircraft aerodynamic behavior. Consequently, rather than opting for a specialized low-Reynolds-number airfoil, it was preferred to use a standard NACA 2415, which features aerodynamic characteristics less sensitive to Reynolds variations, for the expected operative conditions. Second, in view of a possible wind tunnel experimentation to be conducted at the same Reynolds number experience during flight tests, the wingspan was constrained to 1.5 m, a value that could ease the definition of a scaled model to be tested in a wind tunnel owned by the Department of Aerospace Science and Technology of Politecnico di Milano.

DOI: 10.13009/EUCASS2025-515

Figure 1: The Aether two-surface during flight testing.

The wing taper ratio, root incidence angle, and twist were subsequently selected to optimize the lift distribution toward an elliptical profile, at a lift coefficient equal to 0.4.

Dealing with the overall configuration of the airplane, a cylindrical fuselage, low wing, T-tail, pusher configuration with the motor mounted in the tail cone was selected, for multiple reasons. First, the interference between the propeller and the lifting surfaces is minimal; second, the motor does not occupy internal space, and third, it can be easily cooled.

The design of the tail is conducted in an optimization process involving: horizontal tail geometry, mass balancing, CG position, and longitudinal controllability. Once these parameters are determined, the vertical tail is also sized to satisfy different requirements, namely, the directional stability and spin behavior. Both horizontal and vertical surfaces feature a NACA 0012 arfoil. Moreover, the vertical position of the horizontal plane, in the selected T-tail configuration, was defined following the NACA TM-X-26 report indications to avoid the dangerous deep stall occurence.[12]

The control of the Aether is managed by the Pixhawk device and the widespread PX4 autopilot software.[8] The system also integrates a retractable landing gear, off-the-shelf motors for the deflection of control surfaces and an electric motor linked to a propeller to provide for propulsion. The sensor suite consists of a Pitot tube, an inertial measurement unit (accelerometers and gyros), GPS enabling the measurement of the most important flight mechanics variables. Telemetry, batteries and the remote-control unit complete the hardware of the system.

The external shape of the aircraft is 3D-printed and connected to some carbon-fiber-made structural elements which provide stiffness to the system.

Table 1 summarizes the main characteristics of the Aether-Two-surface, while Fig. 1 reports a picture of the Aether two-surface during flight testing.

Wingspan	1.5 m
Wing area	0.314 m^2
Wing taper ratio	0.76
Sweep at quarter chord	3.24 deg
Aspect ratio	7.2 m^2
Max take-off weight	3.5 kg
Airframe weight	2.6 kg
Payload	0.5 kg
Battery weight	0.32 kg
Motor weight	0.08 kg
Battery energy	45.65 Wh
Motor power	300 W

Table 1: Main characteristics of Aether reference two-surface airplane.

DOI: 10.13009/EUCASS2025-515

2.2 Design of the equivalent three-surface airplane

To assess whether a three-surface configuration with redundant longitudinal control represents a viable alternative to conventional aft-tailed designs, a method is proposed to transform an existing two-surface aircraft. The objective is to develop a three-surface variant that achieves improved aerodynamic performance, specifically in terms of maximum lift-to-drag ratio ($E_{\max}$) and power index ($E_{\max}$), while maintaining some peculiar characteristics connected with trim and controllability unaltered.

In this project, we followed the same approach performed in our previous works:[3] we defined an equivalent three-surface airplane with the same wing, with the same static stability margin μ and the same empennage volume V_{emp}. As usual, the static margin is defined as

$$\mu = (x_G - x_N)/c, \tag{1}$$

where x_G and x_N are respectively, the longitudinal position of the center of gravity and the neutral point, c is the mean aerodynamic chord. The longitudinal x-axis originates in the nose of the airplane and points forward.

The neutral point location is defined as usual,

$$x_N = x_G + \frac{C_{m_{G\alpha}}}{C_{L\alpha}}. \tag{2}$$

Although, Eq. (2) is formally identical to the one used for conventional back-tailed airplanes, the derivative $C_{m_{G\alpha}}$ and $C_{L\alpha}$ also account for the presence of the canard in the three-surface configuration.

Finally, the total empennage volume V_{emp} is defined as the sum of the tail V_{tail} and canard volume V_{canard} which can be evaluated through the following equations,

$$V_{\text{tail}} = \frac{S_{\text{T}}\,(x_G - x_{AC_{\text{T}}})}{S\,c} \tag{3}$$

and

$$V_{\text{canard}} = \frac{S_{\text{C}}\,(x_{AC_{\text{C}}} - x_G)}{S\,c}, \tag{4}$$

being $x_{AC_{\text{T}}}$ and $x_{AC_{\text{C}}}$ the location of the aerodynamic centers of the tail and canard surfaces, respectively. In the case of two-surface airplanes, empennage and tail volumes are identical.

The center of gravity position must also be adjusted to account for the changes in configuration when transitioning from the baseline two-surface aircraft to its modified three-surface counterpart. To this end, the weight of both empennages W_{emp} is estimated through the knowledge of the empennage size and the density of the thermoplastic polymers used in the 3D printing.

2.2.1 Optimization of the equivalent three-surface airplane

Through a dedicated process based on Datcom,[5] the constitutive laws of aerodynamic coefficients as functions of the angle of attack α, the elevator deflection δ_E and the canard deflection δ_C, were derived for two-surface airplane and for some candidates three-surface alternatives.

The final expression of the constituive laws of the aerodynamics reads

$$\begin{cases} C_L = & C_{L0} + C_{L\alpha}\alpha + C_{L\delta_{\text{E}}}\delta_{\text{E}} + C_{L\delta_{\text{C}}}\delta_{\text{C}} \\ C_{m_G} = & C_{m_{G}0} + C_{m_{G}\alpha}\alpha + C_{m_{G}\delta_{\text{E}}}\delta_{\text{E}} + C_{m_{G}\delta_{\text{C}}}\delta_{\text{C}} \end{cases} \tag{5}$$

where symbols $C_{\sigma 0}$ and $C_{\sigma\xi}$ represent the constant value of the generic coefficient C_σ, with $\sigma = (L, m_G)$ (lift and pitchin moment reduced to the center of gravity), and its derivative with respect to trim variable $\xi = (\alpha, \delta_E, \delta_C)$. The drag coefficient, on the other hand, features a more complex and nonlinear behavior with respect to the trim variable, which can be formalized as

$$C_D = C_D(\alpha,\, \delta_{\text{E}},\, \delta_{\text{C}}). \tag{6}$$

Equation (6) also considers the interactions among the angle of attack and the deflections of the control surfaces.

The longitudinal trim of an airplane, i.e. the equilibrium of vertical forces and the pitching moments, can be formulated as

$$\begin{cases} C_L = & C_L^* = \frac{W}{qS} \\ C_{m_G} = & 0 \end{cases} \tag{7}$$

where C_L^* is the lift coefficient at trim, S the wing area, W the airplane weight and q the dynamic pressure.

DOI: 10.13009/EUCASS2025-515

C_L and C_{m_G} are expressed as functions of three trim variables α, δ_E and δ_C, hence Eq. (7) represents an undetermined linear system, that can be given a more compact form as

$$\boldsymbol{y} = \boldsymbol{X}\boldsymbol{\xi}, \tag{8}$$

where

$$\boldsymbol{y} = \left\{ \begin{array}{c} C_L^* - C_{L0} \\ -c_{m_{G0}} \end{array} \right\}, \tag{9}$$

$$\xi = \{\alpha,\, \delta_E,\, \delta_C,\, i_\mathrm{T},\, i_\mathrm{C}\}^T, \tag{10}$$

and

$$\boldsymbol{X} = \left[\begin{array}{ccc} C_{L\alpha} & C_{L\delta_E} & C_{L\delta_C} \\ C_{m_{G}\alpha} & C_{m_{G}\delta_E} & C_{m_{G}\delta_C} \end{array} \right]. \tag{11}$$

The indeterminacy of (8) leads to infinite combinations of the trim parameters that satisfy the equilibrium. It is now possible to exploit such an indeterminacy for example to minimize the drag coefficient C_D of the overall airplane for a given lift coefficient $C_L^* = W/(q\,S)$.

The optimal trim problem is then be formalized as a constrained optimization,

$$\boldsymbol{\xi}_\mathrm{trim} = \arg\left(\min\left(C_D(\boldsymbol{\xi})\right)\right) \quad \text{s. t.} \quad \boldsymbol{y} = \boldsymbol{X}\boldsymbol{\xi} \tag{12}$$

that can be solved by standard optimization routines for any C_L and hence for any airplane speed.

The coefficients appearing in Eqs. (5) and (6) represent a parameterized steady flight mechanics model $\mathcal{M}(\boldsymbol{\theta})$, being $\boldsymbol{\theta}$ the array containing all geometry design variables of the three-surface airplane. All parameterized models $\mathcal{M}(\boldsymbol{\theta})$ are also associated with the corresponding optimal drag polar as described previously.

Finally, the design of the three-surface airplane can be formulated as the problem of finding the design parameter array $\boldsymbol{\theta}_\mathrm{opt}$ associated with the maximum lift-to-drag ratio and subjected to the constraint of having the same static margin and empennage volume of a reference two-surface airplane. Accordingly,

$$\boldsymbol{\theta}_\mathrm{opt} = \arg\left(\max\left(E_\mathrm{max}\left(\boldsymbol{\theta}\right)\right)\right) \tag{13a}$$

s. t.

$$\mu(\boldsymbol{\theta}) = \mu_\mathrm{nom} \tag{13b}$$

$$V_\mathrm{total}(\boldsymbol{\theta}) = V_\mathrm{tail\,nom} \tag{13c}$$

being μ_nom and $V_\mathrm{tail\,nom}$ the static margin and the tail volume of the two-surface, airplane.

Following this process and using the area S_C and the incidence i_C of the canard, we found that an optimal three-surface configuration is associated with $S_C = 0.03\,\mathrm{m}^2$ and $i_c = 3\,\mathrm{deg}$.

Fig. 2 shows the upper view of the two airplanes. Both aircraft share the same wing, fuselage, and vertical stabilizer. In the three-surface configuration, the tail size is reduced to compensate for the added canard while maintaining the same total empennage volume, while the wing is slightly shifted rearward to preserve the static margin. Finally, Fig. 3 shows a picture of the Aether three-surface during a flight test.

3. Flight testing definition and results

The flight test campaign began in March 2025, initially focusing on estimating the neutral point of the two-surface reference aircraft. A static margin of 12% was then achieved by placing an appropriate ballast near the aircraft nose. Finally, a series of gliding flights at varying speeds was conducted to allow the quantification of the polar.

The same procedure was applied to the testing of the three-surface aircraft; however, in this case, gliding flights were also performed with varying canard deflections. This resulted in multiple trimmed drag polars, each parameterized by the corresponding canard deflection.

During each gliding flight, the aircraft speed and position were recorded using the pitot tube and GPS, respectively, enabling the estimation of glide angle. Additional measurements were taken to verify that steady flight conditions were maintained throughout the maneuvers.

From the speed measurement, one can readily obtain the lift coefficient as

$$C_L = \frac{2\,W}{qS}, \tag{14}$$

being q and S the dynamic pressure and the wing area.

DOI: 10.13009/EUCASS2025-515

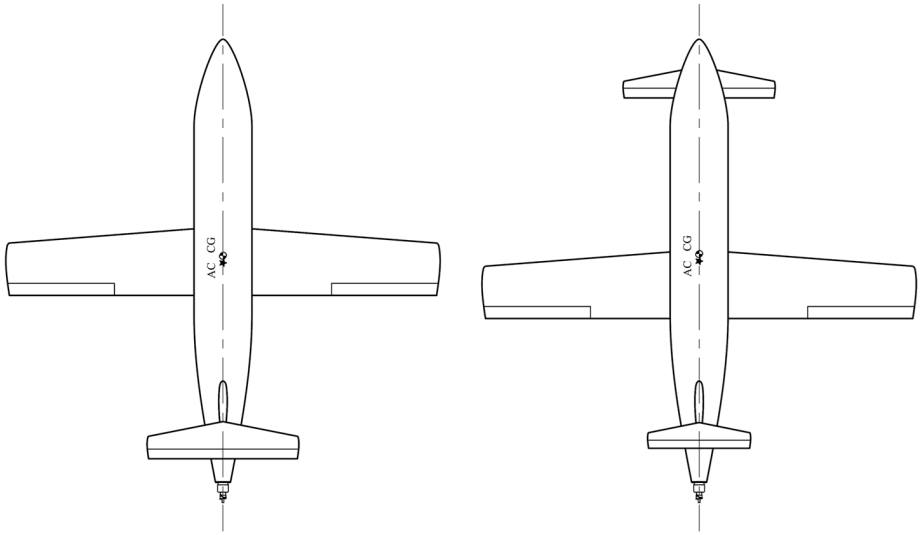

Figure 2: Upper view of the Aether two- and three-surface.

Figure 3: The Aether three-surface during a flight test.

DOI: 10.13009/EUCASS2025-515

Moreover, from the glide angle γ_D, one can compute the lift-to-drag ratio E as

$$E = \frac{1}{\tan(\gamma_D)}. \tag{15}$$

E C_L are finally used for computing the drag coefficient as $C_D = C_L/E$.

Fig. 4 displays the polar data for the two-surface reference airplane (thick dashed black line) and for the three-surface one for three different canard deflections (thin solid lines). Each marker represents the flight data whereas the lines the corresponding quadratic fitting.

Multiple considerations can be derived.

- The three-surface aircraft exhibits lower drag within a range of lift coefficients between 0.25 and 0.7.
- Optimal canard deflections vary across different lift coefficient ranges. For instance, a canard deflection of 12.5 deg yields the best performance between C_L = 0.25 and 0.45, whereas a deflection of 7.5 deg is optimal in the range from C_L = 0.45 and 0.7.
- At low lift coefficients, the two-surface configuration exhibits lower drag. This suggests that the three-surface aircraft with redundant control may be better suited for medium to high lift coefficients.
- The three-surface aircraft with redundant longitudinal control achieves a maximum lift-to-drag ratio that is 10% higher than that of the equivalent two-surface airplane.

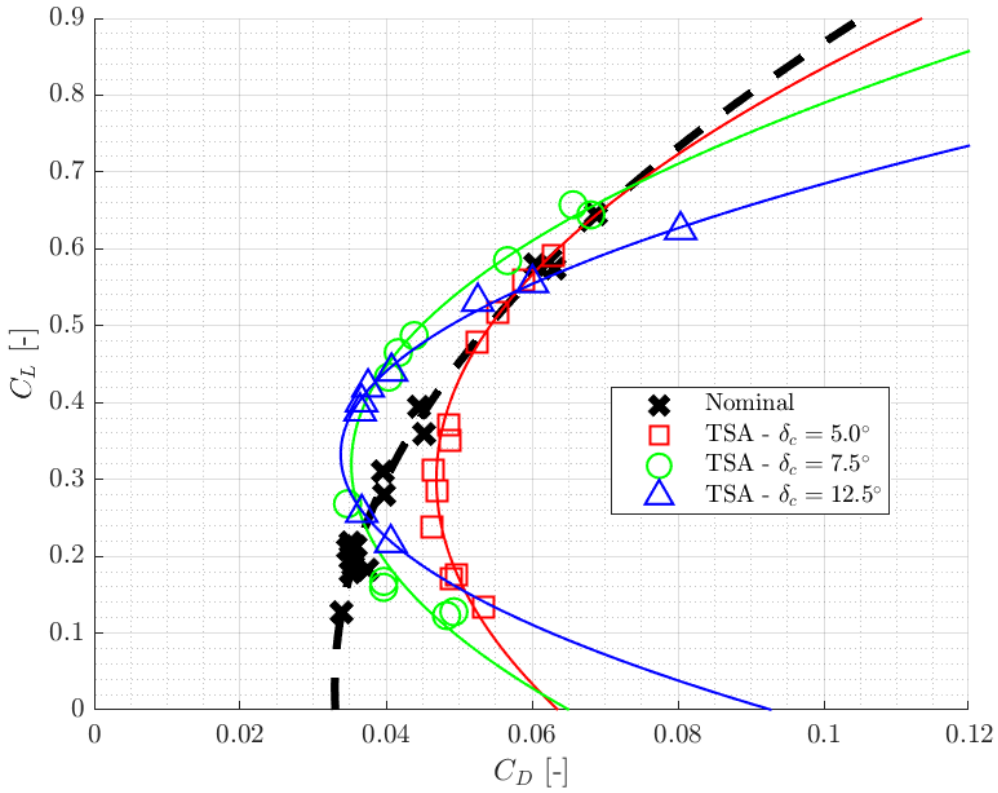

Figure 4: Caption

4. Conclusion

In this paper, we presented ongoing research focused on the analysis of a specific aircraft configuration: the three-surface airplane with redundant longitudinal control. When both the canard and tail are equipped with movable surfaces, the longitudinal trim becomes overdetermined. This redundancy can be leveraged to minimize trimmed drag.

DOI: 10.13009/EUCASS2025-515

To investigate this configuration, we designed and built two remote-controlled aircraft: a reference back-tailed airplane and an equivalent three-surface version featuring redundant longitudinal control. Both models share the same wing, fuselage, static margin, and empennage volume; hence, they can be compared in a first-order approximation.

Data from a flight testing campaign, conducted to characterize the drag polars of both configurations, revealed that the three-surface model achieves a maximum lift-to-drag ratio approximately 10% higher than that of its back-tailed counterpart.

This study provides the first experimental evidence that a three-surface configuration with redundant longitudinal control can deliver improved aerodynamic performance.

These promising results warrant further investigation and expansion. For instance, wind tunnel testing could offer a more controlled and repeatable set of measurements, whereas automated flight could improve the quality of flight testing data.

References

[1] J. W. Agnew and J. R. Hess. Benefits of aerodynamic interaction to the three-surface configuration. *Journal of Aircraft*, 17(11):823–827, 1980.

[2] S. Cacciola, C. Spitale, and C.E.D. Riboldi. Steady analysis of three surface airplanes: Improving the aerodynamic performance through redundant longitudinal control. *34th Congress of the International Council of the Aeronautical Sciences*, pages 1–15, 9–13 September 2024, Florence, Italy.

[3] Stefano Cacciola, Carlo E.D. Riboldi, and Matteo Arnoldi. Three-surface model with redundant longitudinal control: Modeling, trim optimization and control in a preliminary design perspective. *Aerospace*, 8(5), 2021.

[4] Salvatore Corcione, Giordana BonavolontÃ , Agostino De Marco, and Fabrizio Nicolosi. Downwash modelling for three-lifting-surface aircraft configuration design. *Chinese Journal of Aeronautics*, 36(6):161–173, 2023.

[5] R D Fink. Usaf stability and control datcom. Afwal-tr-83-3048, Flight Dynamics Laboratories (AFWAL/FIGC), Air Force Wright Aeronautical Laboratories, Wrigth-Patterson Air Force Base, Ohio 4543, 1978.

[6] Eric R. Kendall. The theoretical minimum induced drag of three-surface airplanes in trim. *Journal of Aircraft*, 22(10):847–854, 1985.

[7] Piaggio P180. Avanti evo. web page: http://www.avantievo.piaggioaerospace.it/.

[8] PX4. Open-source autopilot – for drone developers, https://px4.io/.

[9] Carlo E. D. Riboldi, Stefano Cacciola, and Lorenzo Ceffa. Studying and optimizing the take-off performance of three-surface aircraft. *Aerospace*, 9(3), 2022.

[10] S. Ricci, A. Scotti, and D. Zanotti. Control of an all-movable foreplane for a three surfaces aircraft wind tunnel model. *Mechanical Systems and Signal Processing*, 20(5):1044–1066, 2006.

[11] J. Roskam. *Airplane Design Parts I - VIII: Airplane Design*. DARcorporation, 1997.

[12] Kenneth P. Spreemann. Design guide for pitch-up evaluation and investigation at high subsonic speeds of possible limitations due to wing-aspect-ratio variations. Technical Report NASA TM-X-26, NASA Langley Research Center, Washington, D.C., 1959. Declassified July 11, 1961.

[13] D. Strohmeyer, R. Seubert, W. Heinze, C. Oesterheld, and L. Fornasier. Three surface aircraft - a concept for future transport aircraft. *38th Aerospace Sciences Meeting and Exhibit*, 2000.